The Journal of Pathology: Clinical Research
J Pathol Clin Res July 2021; **7:** 375–384
Published online 26 March 2021 in Wiley Online Library (wileyonlinelibrary.com). DOI: 10.1002/cjp2.208

ORIGINAL ARTICLE

Identification of *NTRK* gene fusions in lung adenocarcinomas in the Chinese population

Ruiying Zhao[1†], Feng Yao[2†], Chan Xiang[1], Jikai Zhao[1], Zhanxian Shang[1], Lianying Guo[1], Wenjie Ding[1], Shengji Ma[1], Anbo Yu[1], Jinchen Shao[1], Lei Zhu[1] and Yuchen Han[1*]

[1]*Department of Pathology, Shanghai Chest Hospital, Shanghai Jiao Tong University, Shanghai, PR China*
[2]*Department of Thoracic Surgery, Shanghai Chest Hospital, Shanghai Jiao Tong University, Shanghai, PR China*

**Correspondence to: Yuchen Han, Department of Pathology, Shanghai Chest Hospital, Shanghai Jiao Tong University, No. 241, West Huai Hai Road, Xv Hui District, Shanghai 200030, PR China. E-mail: ychan@cmu.edu.cn*

[†]*These authors contributed equally to this study.*

Abstract

The molecular profile of neurotrophic tyrosine kinase receptor (*NTRK*) gene fusions in lung adenocarcinoma (LUAD) is not fully understood. Next-generation sequencing (NGS) and pan-tyrosine kinase receptor (TRK) immunohistochemistry (IHC) are powerful tools for *NTRK* fusion detection. In this study, a total of 4,619 LUAD formalin-fixed, paraffin-embedded tissues were collected from patients who underwent biopsy or resection at the Shanghai Chest Hospital during 2017–2019. All specimens were screened for *NTRK1* rearrangements using DNA-based NGS. Thereafter, the cases with *NTRK1* rearrangements and cases negative for common driver mutations were analyzed for *NTRK1/2/3* fusions using total nucleic acid (TNA)-based NGS and pan-TRK IHC. Overall, four *NTRK1/2* fusion events were identified, representing 0.087% of the original sample set. At the DNA level, seven *NTRK1* rearrangements were identified, while only two *TPM3-NTRK1* fusions were confirmed on TNA-based NGS as functional. In addition, two *NTRK2* fusions (*SQSTM1-NTRK2* and *KIF5B-NTRK2*) were identified by TNA-based NGS in 350 'pan-negative' cases. Two patients harboring *NTRK1/2* fusions were diagnosed with invasive adenocarcinoma, while the other two were diagnosed with adenocarcinoma *in situ* and minimally invasive adenocarcinoma. All four samples with *NTRK* fusions were positive for the expression of pan-TRK. The two samples with *NTRK2* fusions showed cytoplasmic staining alone, while the other two samples with *NTRK1* fusions exhibited both cytoplasmic and membranous staining. In summary, functional *NTRK* fusions are found in early-stage LUAD; however, they are extremely rare. According to this study's results, they are independent oncogenic drivers, mutually exclusive with other driver mutations. We demonstrated that NTRK rearrangement analysis using a DNA-based approach should be verified with an RNA-based assay.

Keywords: LUAD; *NTRK*; gene fusion; NGS; pan-TRK

Received 5 August 2020; Revised 9 February 2021; Accepted 14 February 2021

No conflicts of interest were declared.

Introduction

The development of non-small-cell lung cancer (NSCLC) treatment has dramatically progressed since the introduction of epidermal growth factor receptor (*EGFR*) gene mutation and anaplastic lymphoma kinase (*ALK*) gene fusions [1,2]. Recently, the neurotrophic tyrosine kinase receptor (*NTRK*) gene, as an uncommon therapeutic target, has gained more attention. Generally, *NTRK* genes *NTRK1*, *NTRK2*, and *NTRK3* encoding for proteins TRKA, TRKB, and TRKC, respectively, express and function in neuronal development, while gene fusion events have been identified in different types of cancer in both adults and children [3,4]. Tyrosine kinase receptor (TRK) inhibitors such as larotrectinib and entrectinib targeting *NTRK* fusion events have been recently developed and evaluated for treatment efficacy in patients of different ages with various types of cancer [5,6].

NTRK fusion-positive lung adenocarcinoma (LUAD) cases are rare, with an incidence of 0.1–3.3% depending on the analytical setup. Among the three aforementioned TRK genes, *NTRK2* has been rarely reported [6–8]. Nevertheless, these genes represent a

novel 'tissue-agnostic' target, whose therapeutic inhibitors could be potentially applied for the treatment of a broad range of tissue malignancies in clinical trials.

Multiple approaches have been developed to identify *NTRK* fusion at the DNA, RNA, and protein levels. Fluorescence *in situ* hybridization (FISH) [7] with break-apart probes can be employed to detect the occurrence of gene fusions regardless of their fusion partners; however, the application of this approach is constrained by its poor throughput and resolution. Moreover, FISH provides no identity of fusion partners or RNA-level information for therapeutic guidance. In contrast, pan-TRK immunohistochemistry (IHC) has been applied for efficient and reliable *NTRK* fusion screening [9]. The sensitivity and specificity of pan-TRK IHC generally depend on the specific tumor type and gene; a high sensitivity is observed for *NTRK1* and *NTRK2* fusions, and a high specificity for common tumors (lung and colorectal cancers) [10]. Furthermore, next-generation sequencing (NGS) with different targeted gene enrichments can identify divergent genetic events during clinical diagnosis. Hybridization capture-based large DNA panels that simultaneously survey hundreds of genes are particularly powerful in identifying localized mutations; however, they fail to investigate complex genomic translocations with diverse partners and dispersed breakpoints. Amplification-based approaches that utilize sequence-specific primer pairs to enrich targeted regions are challenging; however, they can only detect gene fusions with known fusion partners. RNA-based anchored multiplex polymerase chain reaction (PCR) [11] is specifically tailored for detecting gene fusions through ligation-mediated amplification. Therefore, it is capable of identifying novel fusion events with unknown fusion partners or breakpoints.

To improve *NTRK* fusion detection in LUAD, we conducted this large-scale LUAD cohort study on *NTRK* fusions. Gene fusion events were identified using NGS at both DNA and RNA levels. Meanwhile, pan-TRK IHC was also employed for protein-level gene fusion identification.

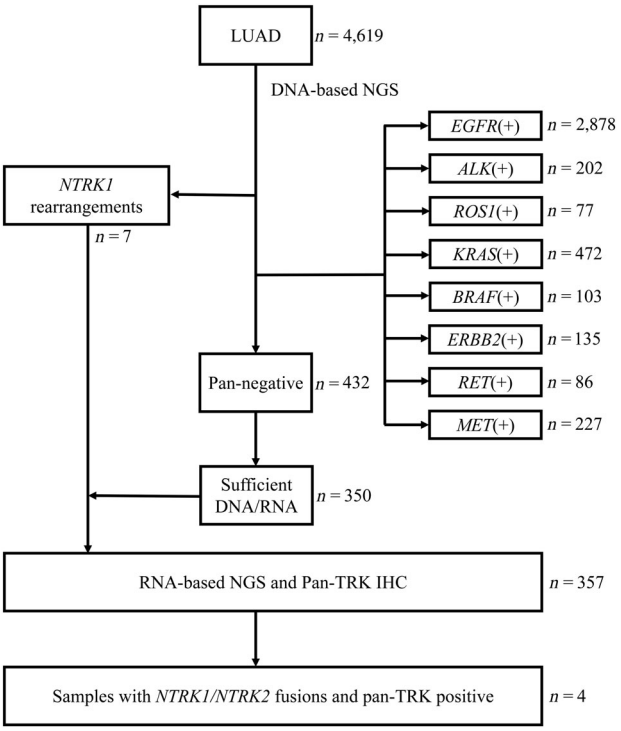

Figure 1. Flow chart of the detection strategy for *NTRK* fusions in LUAD.

Materials and methods

Patient enrollment and sample collection

A total of 4,619 consecutive formalin-fixed, paraffin-embedded (FFPE) LUAD tissues were collected from patients who underwent biopsy or resection at the Shanghai Chest Hospital during 2017–2019 (Figure 1). These samples consisted of 2,651 surgical specimens and 1,968 small biopsies or cell blocks (703 transbronchial biopsies [TBBs], 442 endobronchial ultrasound transbronchial needle aspirations [TBNA], and 823 pleural effusion cell blocks).

The age, sex, specimen types, and histotypes of the 4,619 patients who provided specimens are shown in Table 1. The histotypes were classified according to the 2015 World Health Organization classification scheme for lung carcinoma.

All procedures involving human participants were performed as per the ethical standards of the National Research Committee and the 1964 Helsinki Declaration (including its follow-up amendments and comparable ethical standards). Informed consent was obtained from all the enrolled participants. This study was approved by the Ethics Committee of Shanghai Chest Hospital (#IS2001).

Extraction of DNA/RNA

Genomic DNA was extracted using the QIAamp DNA FFPE Tissue Kit (Qiagen GmbH, Hilden, Germany) according to the manufacturer's instructions. Quantification of the DNA was performed with the Qubit 3.0 dsDNA assay (Life Technologies, Carlsbad, CA,

Table 1. Relationships between *NTRK* fusions and clinicopathological factors.

Factor	Total	*NTRK* fusion
Age (years)		
Mean	58.6	39.25
Median	61	37.5
Range	17–88	31–51
Sex		
Male	2,439	2
Female	2,180	2
Specimen type		
Surgical	2,651	4
Biopsies/cell blocks	1,968	0
Histotype		
AIS	247	1
MIA	412	1
IA	1,992	2

AIS, adenocarcinoma *in situ*; IA, invasive adenocarcinoma; MIA, minimally invasive adenocarcinoma.

USA). The total nucleic acids (TNAs) for the RNA- and DNA-based NGS were prepared differently (see the following subsection 'Unified RNA and DNA NGS based on PANO-Seq').

DNA hybridization capture-based NGS

DNA fragmentation was performed using Covaris M220 (Covaris Inc., Woburn, MA, USA), followed by end repair, phosphorylation, and adaptor ligation. Fragments measuring 200–400 bp in length were selected for further hybridization using capturing probes, magnetic bead enrichment, and PCR amplification.

All samples were subjected to a DNA hybridization capture-based NGS assay as a routine test. The assay is a 68-gene panel covering *NTRK*1/2/3 for all exons and selected introns (Burning Rock Biotech Ltd, Guangzhou, PR China; see supplementary material, Table S1) and is capable of detecting the rearrangement of *NTRK1*. DNA quality and size distribution were assessed using a bioanalyzer. All indexed libraries were sequenced using the NextSeq 550 sequencer (Illumina Inc., San Diego, CA, USA) with paired-end sequencing.

The sequence data were mapped to the human genome (hg19) using BWA aligner 0.7.10. Local alignment optimization, variant calling, and annotation were performed with GATK 3.2, MuTect, and VarScan, respectively. The variants were filtered using the VarScan fpfilter pipeline, with loci with depths <200 filtered out, and then annotated using ANNOVAR and SnpEff v4.3. DNA genomic rearrangement analysis was performed using Factera 1.4.3.

Thereafter, 357 samples were analyzed using TNA-based NGS and pan-TRK IHC, including the cases that carried *NTRK1* rearrangements (seven cases, see Results section). Generally, driver gene mutations occur in LUAD in a mutually exclusive manner. Therefore, for further testing, we selected 350 'pan-negative' samples that did not have common driver gene mutations. The strategy employed to detect *NTRK* fusions is illustrated in Figure 1.

Unified RNA and DNA NGS based on PANO-Seq

The selected cases were analyzed with parallel amplification numerically optimized sequencing (PANO-Seq) [12], using a modified on-shelf product (panel #022T; HeliTec Biotechnologies, Shenzhen, PR China) with atypical *NTRK1/2/3* primers spiked in the multiplexed primer pools. The panel can identify all functional fusion events in multiple common genes and genetic variations in all National Comprehensive Cancer Network (NCCN)-specified biomarkers (see supplementary material, Table S2). To perform this assay, TNA was first extracted from FFPE samples using a PANO-Pure FFPE TNA extraction kit (HeliTec Biotechnologies) and quantified using the Qubit 3.0 dsDNA assay (Life Technologies). Sample quality was determined as pass if DNA was >10 ng/μl and RNA was >25 ng/μl. Then, 50 ng of TNA input was used for library construction. This single-tube library construction protocol used DNA for single nucleotide variant and indel detection, and RNA for fusion detection, as well as tiled intronic primers for DNA-based fusion detection when transcripts were unavailable. The reactions from extraction to sequencing were performed in a single tube as a unified library, without experimentally separating DNA or RNA. Sequencing was performed on an Illumina HiSeq X10 platform with PE150+P7 (8) setting. Raw sequencing data were analyzed using the proprietary PANO-Call ver. 18.12 bioinformatics pipeline for both mutation and fusion calls (HeliTec Biotechnologies).

Pan-TRK IHC

The Ventana pan-TRK (EPR17341) assay (Ventana Medical Systems Inc., Tucson, AZ, USA), in combination with the OptiView DAB IHC Detection Kit (Ventana Medical Systems), was used on the Ventana BenchMark XT automated slide stainer for the detection of TRK A, B, and C. Cortical brain tissue was used as the positive control, while alveolar epithelium was used as a negative internal control. The test results were interpreted by well-trained senior pathologists.

IHC staining was graded according to the percentage of stained tumor cells (0, 0–49, 50–79, or 80–100%) and staining intensity (0, no staining; +, weak; ++, moderate; +++, strong). The staining pattern (cytoplasmic, nuclear, and/or membranous) was also identified. The optimal IHC cut-off was determined according to the NGS and IHC results.

Results

DNA capture-based NGS

In total, *NTRK1* gene rearrangements were identified in seven (0.15%, 7/4,619) patients (cases 1–7; Table 2). Two of these seven *NTRK1* rearrangements (cases 6 and 7) carried both an *NTRK1* kinase domain and a 5' portion of *TPM3*, indicating constitutive transcriptional functions. In contrast, the other five (cases 1–5) carried noncanonical rearrangements, which were without either an *NTRK1* kinase domain or a 5' portion of a partner gene. Moreover, the two samples carrying canonical *TPM3-NTRK1* rearrangements had no detectable concurrent driver mutations, while three of the other five samples carried activating *EGFR* or *KRAS* mutations.

Notably, case 5, who had received EGFR-tyrosine kinase inhibitor (TKI) treatment, was *NTRK1* rearrangement-negative before therapy. Therefore, the noncanonical *NTRK1-FMN2* rearrangement might have been introduced by EGFR-TKI treatment.

Overall, 90.5% (4,180/4,619) of the adenocarcinoma samples possessed known activating mutations of *EGFR* (2,878, 62.31%), *ALK* (202, 4.37%), *ROS1* (77, 1.67%), *KRAS* (472, 10.22%), *BRAF* (103, 2.23%), *RET* (86, 1.86%), *MET* (227, 4.91%), or *ERBB2* (135, 2.92%). In addition to the seven *NTRK1*-rearranged samples, another 432 samples were pan-negative without the aforementioned driver gene mutations.

Parallel amplification numerically optimized sequencing

A total of 357 samples, including 350 pan-negative adenocarcinoma samples and the seven aforementioned *NTRK1* rearranged samples, were selected for PANO-Seq, a concurrent dual-template NGS assay, to confirm the results of DNA-based NGS. The *TPM3-NTRK1* chimeric transcripts of cases 6 and 7 consisted of exon 8 of *TPM3* at the 5' end and *NTRK1* exon 10 at the 3' end at the RNA level, reflecting the partial excision of *NTRK1* exon 9 during splicing in case 6. The other five samples that carried noncanonical *NTRK1* rearrangements were found to have no chimeric *NTRK1* transcripts. In contrast, a *KIF5B-RET* fusion was found at the RNA level in case 1; this was not detected using the former DNA-based NGS assay.

Furthermore, two *NTRK2* fusions were detected at the RNA level (Table 2). One of them, *SQSTM1-NTRK2*, was in an invasive adenocarcinoma sample, and the other *KIF5B-NTRK2* in a minimally invasive adenocarcinoma (MIA) sample. No *NTRK3* fusions were found in these samples.

Pan-TRK IHC

Pan-TRK IHC testing was further performed on the 357 aforementioned samples to examine TRK A, B, and C expression. The IHC results are summarized in Table 3. Weak, moderate, or strong cytoplasmic staining was observed in 13 cases, and 2 of these also had moderate membranous staining. All staining was observed in 80–100% of tumor cells. The four *NTRK* fusion cases detected using TNA-based NGS had moderate to strong cytoplasmic staining, and two of them also had moderate membranous staining. Therefore, the optimal cut-off was moderate to strong cytoplasmic staining in 80–100% of tumor cells with or without other subcellular staining patterns. The cells with *NTRK2* fusions showed cytoplasmic staining only, while those with *NTRK1* fusions were positive for both cytoplasmic and membranous staining (Figure 2).

Discussion

In this study, we identified four *NTRK* gene fusions in 4,619 LUAD samples (0.087%). Two of them were *TPM3-NTRK1* fusions that were identified using DNA- and RNA-based NGS and confirmed using pan-TRK IHC. The other two were *SQSTM1-NTRK2* and *KIF5B-NTRK2* fusions, which were detected using RNA-based NGS and confirmed using pan-TRK IHC. However, we identified two *NTRK* fusions, *TPM3-NTRK1* (in adenocarcinoma *in situ* [AIS]) and *KIF5B-NTRK2* (in MIA) in the early stage of adenocarcinoma. This finding was different from previous studies that identified such fusion events in advanced adenocarcinoma, and preferentially in mucinous carcinoma or poorly differentiated cells [6,8,11]. Our findings thus extend the understanding of pathological features of *NTRK* gene fusions in LUAD. In addition, to the best of our knowledge, *NTRK* fusions in NSCLC are dominated by *NTRK1* and *NTRK3* fusions, with only one

Table 2. *NTRK* fusion detected using NGS at DNA and RNA levels and pan-TRK IHC at the protein level.

Case no.	Sex	Age (years)	Smoking (pack-years)	Pathological stage	Specimen type	Histotype	Tumor size (cm)	DNA rearrangement	RNA fusion	Pan-TRK	Other drivers
1	M	53	0	T1cN0M0 IA	Small biopsy	ADC	2.7	*C14orf2-NTRK1* (intergenic: intron 11)	*KIF5B-RET* (exon 15–exon 12)	–	
2	M	41	0	T1bN0M0 IA	Surgical	PPA	1.8	*RRNAD1-NTRK1* (UTR3-exon 15)	–	–	*EGFR* L858R
3	F	64	0	T1bN0M0 IA	Surgical	APA	1.5	*NTRK1-NBPF25P* (intron 8-intergenic)	–	–	
4	M	54	30	T2aN3M1 IV	Small biopsy	ADC	2	*NTRK1-ARHGEF11* (exon 17: intron 1)	–	–	*KRAS G12A*
5	F	56	0	T4N3M1 IV	Small biopsy	ADC	1	*NTRK1-FMN2* (intron 11: intron 16)	–	–	*EGFR* 19del
6	F	31	0	T1aN0M0 IA	Surgical	AIS	0.8	*TPM3-NTRK1* (intron 8: exon 9)	*TPM3-NTRK1* (exon 8–exon 10)	+ Cytoplasmic	
7	M	51	0	T1bN0M0 IA	Surgical	PPA	1.5	*TPM3-NTRK1* (intron 8: intron 9)	*TPM3-NTRK1* (exon 8–exon 10)	+ Cytoplasmic	
8	F	39	0	T1cN2M0 IIIA	Surgical	APA	2.5	–	*SQSTM1-NTRK2* (exon 4–exon 15)	+ Cytoplasmic membranous	
9	M	36	0	T1aN0M0 IA	Surgical	MIA	1.3	–	*KIF5B-NTRK2* (exon 24–exon 15)	+ Cytoplasmic membranous	

One pack-year is equal to smoking 20 cigarettes (1 pack) per day for 1 year.
ADC, adenocarcinoma; AIS, adenocarcinoma *in situ*; APA, acinar-predominant adenocarcinoma; F, female; M, male; MIA, minimally invasive adenocarcinoma; PPA, papillary-predominant invasive adenocarcinoma

Table 3. Summary of pan-TRK IHC staining results.

	Total	0	1+	2+	3+
Cytoplasmic	13*	344	9	3	1
Membranous	2*	355	0	2	0
Nuclear	0	357	0	0	0

*Percentage of all tumor cells with staining = 80–100%.

case of *NTRK2* fusion (*SQSTM1-NTRK2*) identified in previous studies [3]. Thus, this research suggests that the *NTRK2* fusion might be underestimated in LUAD. It is generally recognized that driver gene fusions occur more frequently in younger patients than in older patients. Compared with that in *ALK* [13] and *ROS1* [14] cohorts, the mean age was younger in this *NTRK1/2* fusion cohort (*NTRK* versus *ALK* versus *ROS1*: 39.25 versus 54.60 versus 56.09). However, as none of the four patients carrying *NTRK* fusions received larotrectinib or entrectinib therapy, the efficacy of these *NTRK* fusions on corresponding inhibitors could not be assessed.

The coexistence of *NTRK* fusions with other driver gene mutations remains controversial. In this study, we demonstrated that *NTRK* fusions and other known driver gene mutations were mutually exclusive. This finding is similar to that of Hechtman *et al* on solid cancers in 2017 [9]. In contrast, Xia *et al* suggested that the *NTRK1* gene fusion serves as one of the resistance mechanisms for EGFR-TKI in patients with *EGFR*-mutated NSCLC [15], indicating that the *NTRK1* fusion can be concurrent with *EGFR* mutations. In the present study, we detected one *NTRK1* rearrangement using DNA-based NGS in a patient who received EGFR-TKI therapy and later developed TKI resistance (case 5; Table 2); however, this *NTRK1-FMN2* rearrangement contained no *NTRK1* kinase domain. Therefore, we speculate that therapeutic pressure and tumor microenvironment might be responsible for this nonfunctional *NTRK1* rearrangement, while a functional *NTRK* fusion, as an independent driver, is more likely to occur in a mutually exclusive pattern.

Pan-TRK IHC was performed to detect the expression of TRK A, B, and C. With an optimal cut-off, pan-TRK IHC indicated 100% sensitivity and specificity in this study. Therefore, cases with diffuse moderate to strong cytoplasmic staining were identified as pan-TRK-positive in LUAD. However, the positive results should be validated using an RNA-based NGS assay, considering the limited number of positive cases in this study and the weak pan-TRK expression in some *NTRK* fusion-negative cases.

The subcellular localization of different types of gene fusions correlates with the characteristics of fusion partners, indicates various kinase inhibitor effects (ROS1 fusion) [16], and leads to different staining patterns. Therefore, different staining patterns must be studied. We identified both cytoplasmic and membranous staining patterns for the two *TPM3-NTRK1* fusions, while *SQSTM1-NTRK2* and *KIF5B-NTRK2* only exhibited cytoplasmic staining, which is partially attributed to the characteristics of the fusion partners. *TPM3* encodes tropomyosins that participate in cytoskeleton formation in nonmuscle cells and localizes to the cell membrane. *SQSTM1* encodes sequestosome-1, an autophagosome cargo protein localized to the cytoplasm. *KIF5B* encodes kinesin, which is required for normal mitochondria and lysosome distribution, and localizes to the cytoplasm. In addition, we found that the staining intensities of *TPM3-NTRK1* fusions differed in different LUAD histotypes in this study and were different from that of the same fusion type in colorectal carcinoma [3]. Moreover, the staining pattern of the *SQSTM1-NTRK2* fusion also differed in this study and a previous report [3]. Hence, it is suggested that the staining patterns of pan-TRK were simultaneously influenced by various factors, such as fusion partners, tumor type, and cancer histotypes.

Among the seven cases of *NTRK1* rearrangement detected using DNA-based NGS, only two *TPM3-NTRK1* fusions were supported by clear RNA-template evidence using TNA-based NGS, including in-frame exonic breakpoint and strong expression. Others are likely nonfunctional owing to a disrupted kinase domain and lack of RNA-level support. Driver gene mutations (*KIF5B-RET* fusion, *EGFR* L858R mutation, *KRAS* G12A mutation, and *EGFR* exon 19 deletion) with clear functional and clinical significance coexisted in four patients that carried noncanonical rearrangements, further implying that these noncanonical *NTRK* rearrangements are unlikely to be oncogenic. Furthermore, TNA-based NGS found two *NTRK2* fusions, which were difficult to detect using DNA-based NGS because of the difficulty in tiling entire introns. Meanwhile, DNA-based NGS failed to identify canonical *KIF5B-RET* fusion events in case 1, which further highlights the importance of RNA-based approaches for gene fusion detection.

In general, fusion events involve DNA-, RNA-, and protein-level changes. At the DNA level, gene rearrangements may be induced by genomic insertion, deletion, inversion, or amplification, and can be either intra- or inter-chromosomal [17,18]. For example, inverted translocation (in case 6) can potentially generate reciprocal gene rearrangements (Figure 3A), which may complicate the results of DNA-based NGS.

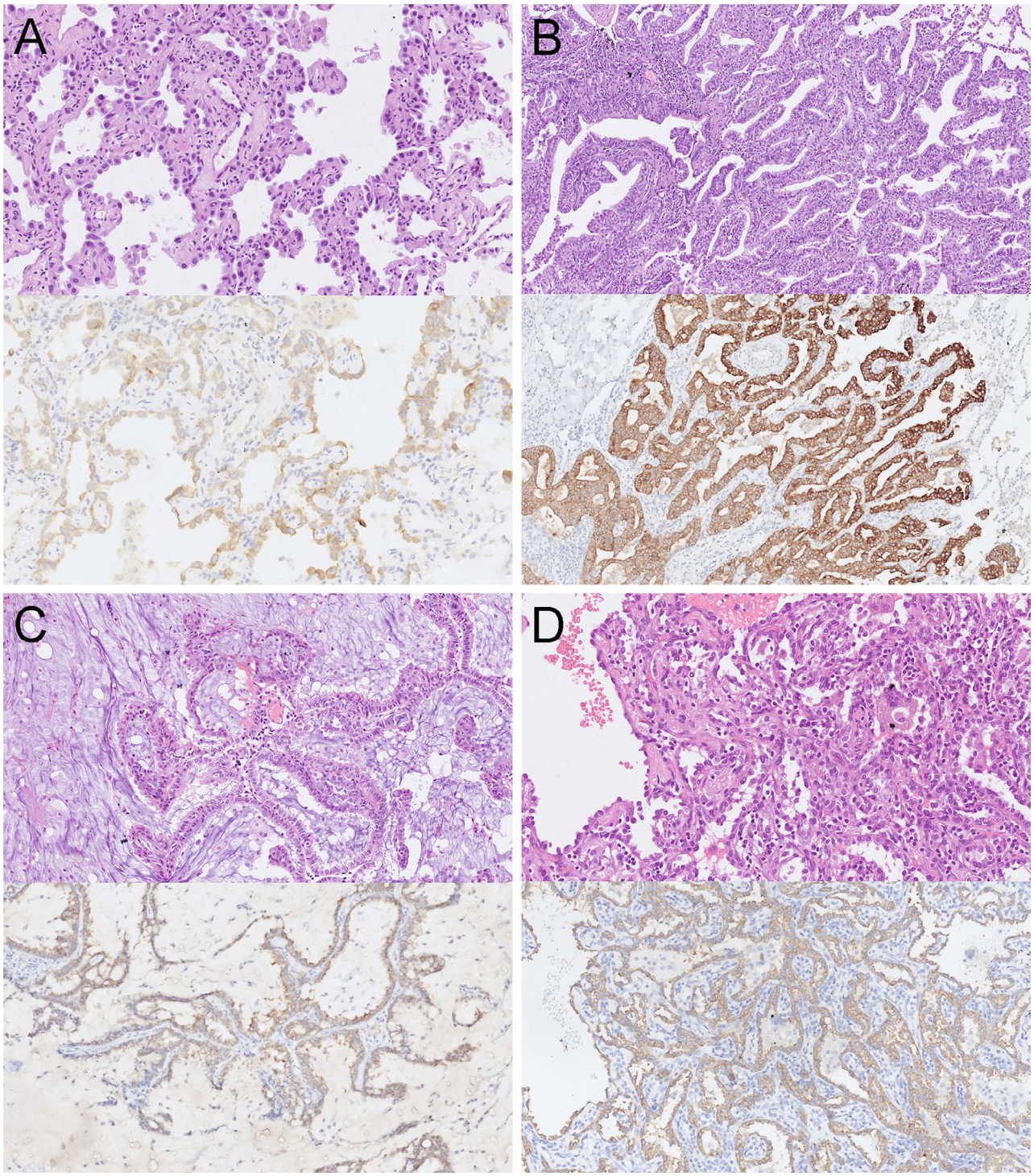

Figure 2. Histotypes of the four samples harboring *NTRK* fusions and the staining patterns of their corresponding pan-TRK IHC results. (A) AIS, *TPM3-NTRK1*, moderate cytoplasmic staining (2+). (B) Papillary-predominant invasive adenocarcinoma, *TPM3-NTRK1*, strong cytoplasmic staining (3+). (C) Acinar-predominant adenocarcinoma, *SQSTM1-NTRK2*, moderate cytoplasmic and membranous staining (2+). (D) MMIA, *KIF5B-NTRK2*, moderate cytoplasmic and membranous staining (2+).

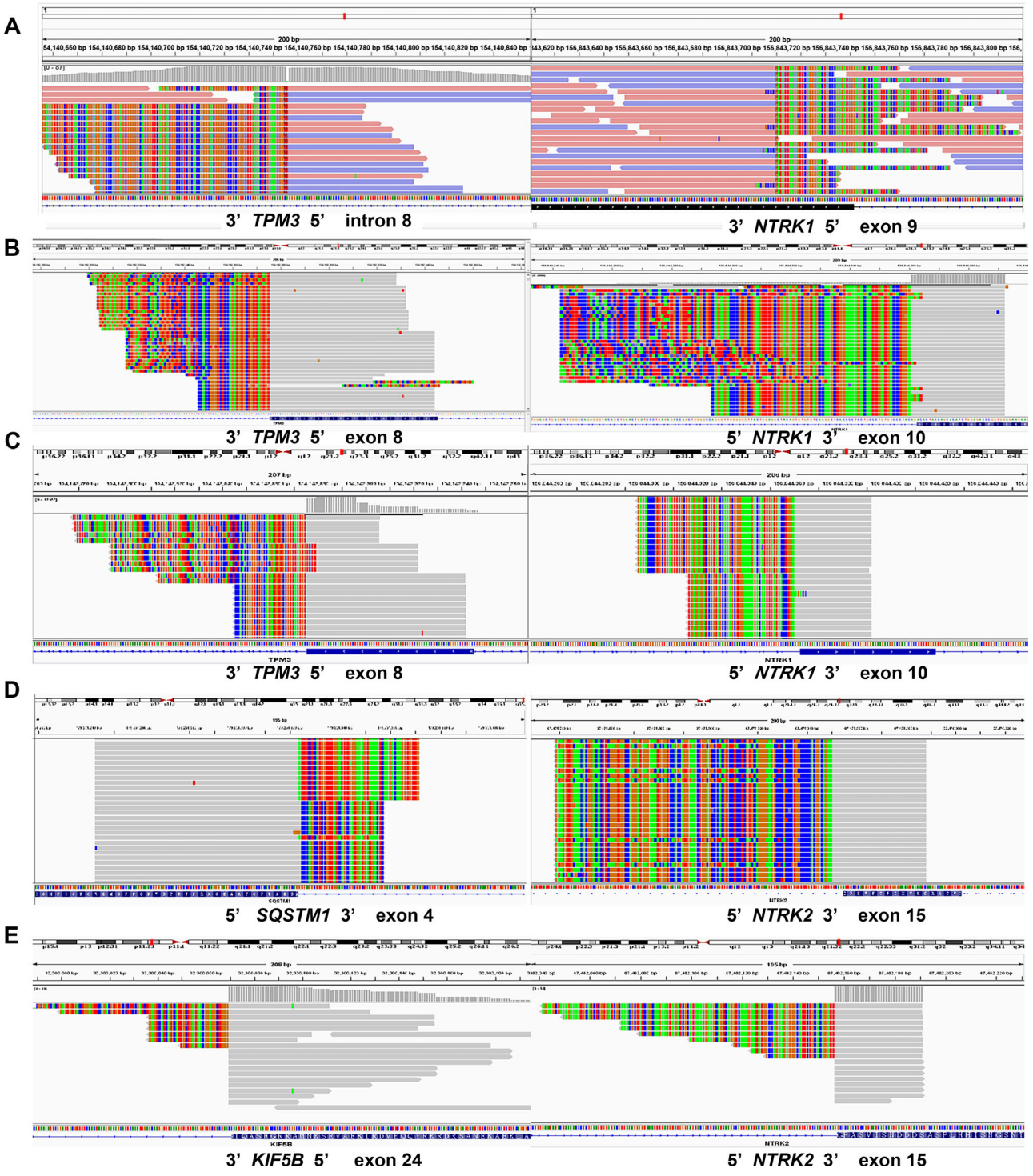

Figure 3. Integrative Genomics Viewer screenshot of *NTRK* genes and corresponding fusion partners detected using NGS. (A) *TPM3-NTRK1* rearrangement in case 6 detected using DNA-based NGS with visible bidirectional chimeric reads. (B) *TPM3-NTRK1* fusion in case 6 detected using RNA-based NGS. (C) *TPM3-NTRK1* fusion in case 7 detected using RNA-based NGS. (D) *SQSTM1-NTRK2* fusion in case 8 detected using RNA-based NGS. (E) *KIF5B-NTRK2* fusion in case 9 detected using RNA-based NGS.

Genomic alterations and transcriptional abnormalities are not always identical. Previously, *EML4-ALK* transcripts were identified at the RNA level in four patients harboring only nonfunctional *ALK* rearrangements [13], which might be formed through uncommon or unknown mechanisms [19]. At the protein level, IHC-positive results can be attributed to either gene fusion events [20] or other forms of abnormalities such as *ALK* alternative transcription initiation, which generates oncoproteins with kinase activities [21]. Considering the aforementioned discrepancy among genetic information, transcriptional changes, and protein functions, a combined application of DNA-, RNA-, and protein-level methods are recommended for identifying gene fusion events.

Many studies have indicated a similar testing algorithm for *NTRK* fusion in solid cancers; this algorithm suggested a combined strategy using IHC and NGS assays for detecting *NTRK* fusion in lung cancer [22–26]. For example, the European Society for Medical Oncology Translational Research and Precision Medicine Working Group recommended using targeted NGS panels (either DNA- or RNA-based) to detect *NTRK* fusions and confirming the positive samples using pan-TRK IHC; a reverse strategy can be adopted as well, if no frontline NGS platform is available [22]. Based on our findings, we recommend detecting *NTRK* fusions in LUAD FFPE samples using DNA-based NGS and identifying the nonfunctional rearrangements using RNA-based NGS or IHC. Furthermore, RNA-based approaches, followed by IHC confirmation with corresponding antibodies, or vice versa, are recommended for LUADs without common driver gene mutations. Although similar studies have been recently published [27,28], more comprehensive investigations remain essential to examine the efficiency of the recommended detection approaches.

We also performed pan-TRK IHC on 60 pan-negative lung squamous cell carcinoma cases without the aforementioned driver mutations. Four cases (6.67%, 4/60) had diffuse moderate (2+) cytoplasmic staining, which is identified as 'pan-TRK-positive' using the above cut-off in LUAD. Three other cases (5.0%, 3/60) had diffuse weak (1+) cytoplasmic staining. All seven of these cases were investigated using TNA-based NGS, but negative results were obtained. Therefore, pan-TRK expression in lung squamous cell carcinoma should be treated more cautiously; it tends to be negative for *NTRK* fusion.

In addition, among the 432 pan-negative adenocarcinoma samples, 198 were surgical tissues and 234 were small biopsies or cell blocks (83 TBB samples, 55 TBNA samples, and 96 pleural effusion cell blocks). All surgical samples had sufficient tissue to be detected using PANO-Seq and pan-TRK IHC, while 35% (82/234) of small biopsy/cell block samples had insufficient tissue for further testing. Therefore, for small specimens without enough tissue for multiple testing, an RNA- or TNA-based NGS assay should be used for fusion detection.

In conclusion, functional *NTRK* fusions are extremely rare in LUAD. *NTRK* fusions may occur at the early stage of LUAD, such as in AIS and MIA. Functional *NTRK* fusion is an independent driver that occurs in a mutually exclusive manner with other driver mutations. Moreover, we recommend detecting *NTRK* rearrangements using DNA-based NGS, followed by RNA-based verification, while pan-TRK IHC is another applicable approach for *NTRK* fusion detection in LUAD. IHC results with pan-TRK expression should be validated using NGS assays.

Acknowledgements

The authors acknowledge Dr Li Chen (HeliTec Biotechnologies) for reviewing the manuscript. The authors acknowledge HeliTec Biotechnologies and Burning Rock Biotech Ltd for technical support. We would like to thank Wiley editing services for English language editing of this manuscript. This work was supported by the Interdisciplinary Program of Shanghai Jiao Tong University (project number ZH2018QNA66) and the Shanghai Municipal Commission of Health and Family Planning (grant number 2018ZHYL0213).

Author contributions statement

RZ and FY were involved in study design, data analysis, data interpretation, and writing of the manuscript. CX, JZ, ZS, LG, WD, SM, AY, JS and LZ carried out the experiments and collected and analyzed the data. YH was involved in study conception and design, pathology assessment, and article revision. All authors were involved in writing the paper and had final approval of the submitted and published versions.

Data availability statement

The datasets generated and/or analyzed during the current study are available from the corresponding author on reasonable request.

References

1. Maemondo M, Inoue A, Kobayashi K, *et al*. Gefitinib or chemotherapy for non-small-cell lung cancer with mutated *EGFR*. *N Engl J Med* 2010; **362:** 2380–2388.
2. Soda M, Choi YL, Enomoto M, *et al*. Identification of the transforming *EML4–ALK* fusion gene in non-small-cell lung cancer. *Nature* 2007; **448:** 561–566.
3. Gatalica Z, Xiu J, Swensen J, *et al*. Molecular characterization of cancers with *NTRK* gene fusions. *Mod Pathol* 2019; **32:** 147–153.
4. Laetsch TW, DuBois SG, Mascarenhas L, *et al*. Larotrectinib for paediatric solid tumours harbouring *NTRK* gene fusions: phase 1 results from a multicentre, open-label, phase 1/2 study. *Lancet Oncol* 2018; **19:** 705–714.
5. Drilon A, Laetsch TW, Kummar S, *et al*. Efficacy of larotrectinib in TRK fusion–positive cancers in adults and children. *N Engl J Med* 2018; **378:** 731–739.
6. Farago AF, Le LP, Zheng Z, *et al*. Durable clinical response to entrectinib in *NTRK1*-rearranged non-small cell lung cancer. *J Thorac Oncol* 2015; **10:** 1670–1674.
7. Vaishnavi A, Capelletti M, Le AT, *et al*. Oncogenic and drug-sensitive *NTRK1* rearrangements in lung cancer. *Nat Med* 2013; **19:** 1469–1472.
8. Farago AF, Taylor MS, Doebele RC, *et al*. Clinicopathologic features of non–small-cell lung cancer harboring an *NTRK* gene fusion. *JCO Precis Oncol* 2018; **2018:** PO.18.00037.
9. Hechtman JF, Benayed R, Hyman DM, *et al*. Pan-Trk immunohistochemistry is an efficient and reliable screen for the detection of *NTRK* fusions. *Am J Surg Pathol* 2017; **41:** 1547–1551.
10. Solomon JP, Linkov I, Rosado A, *et al*. NTRK fusion detection across multiple assays and 33,997 cases: diagnostic implications and pitfalls. *Mod Pathol* 2020; **33:** 38–46.
11. Zheng Z, Liebers M, Zhelyazkova B, *et al*. Anchored multiplex PCR for targeted next-generation sequencing. *Nat Med* 2014; **20:** 1479–1484.
12. Song Z, Xu C, He Y, *et al*. Simultaneous detection of gene fusions and base mutations in cancer tissue biopsies by sequencing dual nucleic acid templates in unified reaction. *Clin Chem* 2020; **66:** 178–187.
13. Zhao R, Zhang J, Han Y, *et al*. Clinicopathological features of *ALK* expression in 9889 cases of non-small-cell lung cancer and genomic rearrangements identified by capture-based next-generation sequencing: a Chinese retrospective analysis. *Mol Diagn Ther* 2019; **23:** 395–405.
14. Zhang Q, Wu C, Ding W, *et al*. Prevalence of ROS1 fusion in Chinese patients with non-small cell lung cancer. *Thorac Cancer* 2019; **10:** 47–53.
15. Xia H, Xue X, Ding H, *et al*. Evidence of NTRK1 fusion as resistance mechanism to EGFR TKI in EGFR+ NSCLC: results from a large-scale survey of NTRK1 fusions in Chinese patients with lung cancer. *Clin Lung Cancer* 2020; **21:** 247–254.
16. Neel DS, Allegakoen DV, Olivas V, *et al*. Differential subcellular localization regulates oncogenic signaling by ROS1 kinase fusion proteins. *Cancer Res* 2019; **79:** 546–556.
17. Kumar-Sinha C, Kalyana-Sundaram S, Chinnaiyan AM. Landscape of gene fusions in epithelial cancers: seq and ye shall find. *Genome Med* 2015; **7:** 129.
18. Rosenbaum JN, Bloom R, Forys JT, *et al*. Genomic heterogeneity of *ALK* fusion breakpoints in non-small-cell lung cancer. *Mod Pathol* 2018; **31:** 791–808.
19. Jividen K, Li H. Chimeric RNAs generated by intergenic splicing in normal and cancer cells. *Genes Chromosomes Cancer* 2014; **53:** 963–971.
20. Du Z, Lovly CM. Mechanisms of receptor tyrosine kinase activation in cancer. *Mol Cancer* 2018; **17:** 58.
21. Wiesner T, Lee W, Obenauf AC, *et al*. Alternative transcription initiation leads to expression of a novel *ALK* isoform in cancer. *Nature* 2015; **526:** 453–457.
22. Marchiò C, Scaltriti M, Ladanyi M, *et al*. ESMO recommendations on the standard methods to detect NTRK fusions in daily practice and clinical research. *Ann Oncol* 2019; **30:** 1417–1427.
23. Penault-Llorca F, Rudzinski ER, Sepulveda AR. Testing algorithm for identification of patients with TRK fusion cancer. *J Clin Pathol* 2019; **72:** 460–467.
24. Hsiao SJ, Zehir A, Sireci AN, *et al*. Detection of tumor NTRK gene fusions to identify patients who may benefit from tyrosine kinase (TRK) inhibitor therapy. *J Mol Diagn* 2019; **21:** 553–571.
25. Pfarr N, Kirchner M, Lehmann U, *et al*. Testing NTRK testing: wet-lab and in silico comparison of RNA-based targeted sequencing assays. *Genes Chromosomes Cancer* 2020; **59:** 178–188.
26. Naito Y, Mishima S, Akagi K, *et al*. Japan Society of Clinical Oncology/Japanese Society of Medical Oncology-led clinical recommendations on the diagnosis and use of tropomyosin receptor kinase inhibitors in adult and pediatric patients with neurotrophic receptor tyrosine kinase fusion-positive advanced solid tumors, cooperated by the Japanese Society of Pediatric Hematology/Oncology. *Int J Clin Oncol* 2020; **25:** 403–417.
27. Benayed R, Offin M, Mullaney K, *et al*. High yield of RNA sequencing for targetable kinase fusions in lung adenocarcinomas with no mitogenic driver alteration detected by DNA sequencing and low tumor mutation burden. *Clin Cancer Res* 2019; **25:** 4712–4722.
28. Pan Y, Zhang Y, Ye T, *et al*. Detection of novel NRG1, EGFR, and MET fusions in lung adenocarcinomas in the Chinese population. *J Thorac Oncol* 2019; **14:** 2003–2008.

SUPPLEMENTARY MATERIAL ONLINE

Table S1. Gene list of DNA hybridization capture-based NGS

Table S2. Gene list of the PANO-Seq